ASEAN Journal of Chemical Engineering 2026, Vol. 26, No. 1, 59 – 70

Removal of Chloride in Saline Water by Bismuth Oxide Nanoparticles

Nguyen Trung Thanh [1,2]
Le Thanh Thien [2,3]
Nguyen Thi Thuy [2,4]
Ho Lien Hue [2,6]
Le Tri Thich [1,2]
Surapol Padungthon [5]
Phan Phuoc Toan [2,6],
Nguyen Thi Quynh Anh [1,2,7]
Nguyen Nhat Huy [*,2,7]

[1] *Laboratory of Nanomaterial, An Giang University, 18 Ung Van Khiem St., Long Xuyen Ward, An Giang Province, Vietnam*
[2] *Vietnam National University Ho Chi Minh City, Vo Truong Toan Street, Linh Xuan Ward, Ho Chi Minh City, Vietnam*
[3] *Institute for Environment and Resources, 142 To Hien Thanh St., Dien Hong Ward, Ho Chi Minh City, Vietnam*
[4] *School of Chemical and Environmental Engineering, International University, Quarter 33, Linh Xuan Ward, Ho Chi Minh City, Vietnam*
[5] *Department of Environmental Engineering, Khon Kaen University, 123 Moo 16 Mittraphap Rd., Nai-Muang, Muang District, Khon Kaen 40002, Thailand*
[6] *Faculty of Engineering - Technology - Environment, An Giang University, 18 Ung Van Khiem St., Long Xuyen Ward, An Giang Province, Vietnam*
[7] *Faculty of Environment and Natural Resources, Ho Chi Minh City University of Technology (HCMUT), 268 Ly Thuong Kiet St., Dien Hong Ward, Ho Chi Minh City, Vietnam*
*e-mail: nnhuy@hcmut.edu.vn

Submitted 10 March 2025 *Revised* 19 December 2025 *Accepted* 19 March 2026

Abstract. Climate change intensifies saltwater intrusion in coastal and delta regions, notably the Mekong Delta, thereby increasing the concentration of chloride ions (Cl^-) in water. Elevated Cl^- concentrations pose serious environmental challenges, inhibiting plant growth and impacting human health. While various conventional methods for chloride treatment exist, challenges persist concerning high cost, complex procedures, and secondary waste. Therefore, developing a simple, cost-effective, and highly efficient method using novel adsorbent materials is imperative. The primary objective of this study was to prepare and evaluate the efficacy of bismuth oxide nanoparticles (Bi_2O_3) as a novel, highly effective adsorbent for the removal of Cl^- from saline water sources. Bi_2O_3 nanoparticles were synthesized using the solid dispersion evaporation technique with sorbitol as a support. FTIR, XRD, SEM, and EDX were used to characterize the physicochemical and structural properties of the material. The Cl^- removal capacity was systematically studied under diverse operational conditions, including contact time, solution pH, adsorbent dosage, initial Cl^- concentration, and temperature, to determine appropriate adsorption conditions. The material was also subjected to adsorption-desorption cycling tests to evaluate its regeneration potential and long-term durability. The kinetic study showed that the Bi_2O_3 material reached adsorption

DOI: 10.22146/ajche.20270

equilibrium efficiently after 90 minutes. The maximum Cl^- adsorption capacity was 40.89 mg/g at an optimum solution pH of 4, under optimized conditions (initial Cl^- concentration of 50 mg/L, 25 °C). Other investigated factors significantly influenced the adsorption kinetics and capacity. Crucially, the Bi_2O_3 adsorbent maintained its high removal efficiency over 10 regeneration cycles, confirming its excellent durability and potential for real-world applications. The results clearly demonstrate that the synthesized Bi_2O_3 nanoparticles have excellent potential as a robust, high-performing adsorbent for Cl^- removal, suggesting a viable and practical solution to the challenges posed by saltwater intrusion.

Keywords: Adsorption, Bi_2O_3, Chloride, Desalination, Saline Water, Water Treatment

INTRODUCTION

Mekong Delta is one of the key center of agriculture in Vietnam, but it has been under heavy impaction of climate change and sea level rise (T. T. Be *et al.,* 2007; Phuong *et al*., 2009) and is suffered by the less freshwater resources due to the saline intrusion (N. V. Be *et al*., 2017; T. T. Be *et al.*, 2007). Before 1995, the Mekong's coastal areas were generally severely affected by salinization during the dry season (Binh *et al.*, 2012). Also, salinization could influence rice or bagasse yield; it was more pronounced with late rains or a longer dry season (Binh *et al*., 2012). From 2000 to 2016, according to the MIKE11 model, saline intrusion in Ben Tre province showed an increasing trend in the first half of the year (Dao & Binh, 2019). At the end of 2019, salinization often occurred at a high rate with 4 g/L.

Additionally, Ben Tre was the first place to suffer from salinization in the last month of 2019. In the estuaries of the Mekong River, salinization reached a depth of 57 km (Ham Luong River), which was 24 km deeper than the long-term average and 17 km deeper than in 2015 (Vo & Son, 2022). According to the research by Hoa *et al.* (2016), rice and shrimp farms in Ben Tre province had salinities exceeding 10‰. Additionally, the paddy fields in An Giang province and Ben Tre province suffered severe saltwater intrusion. To fully comprehend the impact of this phenomenon on the region, it is essential first to establish a precise scientific definition and a method for measuring water salinity.

For more information, salinity was denoted as S‰ (S stands for salinity - salinity) and the total amount (in grams) of dissolved substances contained in 1 kg of water (N. V. Be *et al.,* 2017; Binh *et al.,* 2012; Rahaman *et al.,* 2020; Vengosh, 2014). In oceanography, salinity was used to characterize the minerality of seawater because the total concentration of major ions (11 ions, including Na^+, Ca^{2+}, Mg^{2+}, Fe^{3+}, NH_4^+, Cl^-, SO_4^{2-}, HCO_3^-, CO_3^{2-}, NO_2^-, and NO_3^-) accounts for 99.99% of the total amount of dissolved minerals (N. V. Be *et al.*, 2017; Binh *et al.*, 2012; Vengosh, 2014). Therefore, the salinity of seawater could be considered equal to the sum of dissolved minerals in 1 gram of seawater. It also means that salinity could be calculated through the concentration of any one major ion in seawater. Consequently, the increasing presence of these dissolved substances, particularly the highly concentrated chloride ions, presents immediate and severe risks to ecosystems and public health.

High salinity in water affects animals, plants, humans, and the environment. Specifically, plants affected by salinity

exhibited symptoms such as leaf burning, leaf yellowing, defoliation of flowers and fruits, reduced growth and development, and reduced crop yield (Queensland Government, 2013). Moreover, when high-salt content enters the body, it increases the permeability of cell membranes. Sodium ions will enter smooth muscle cells of the vessel wall, increasing cell water content and vascular tone, increasing peripheral resistance, and leading to hypertension, stroke, and cardiovascular disease (Queensland Government, 2013; Rahaman *et al.,* 2020). Besides, chloride in saline water increases the water's electrical conductivity and corrodes metal devices. Saline water, especially chloride, was extremely toxic to plants, causing death and poisoning (Queensland Government, 2013). Addressing these severe environmental and public health threats requires the development of effective, cost-efficient, and easily deployable water treatment technologies capable of selectively removing chloride.

Given this serious problem, many methods for reducing saline intrusion and removing chloride from water have been developed. The most common methods are ion exchange, RO purifier, traditional distillation method, biological method, or membrane technology. In general, these methods involve complex operating procedures, high operating costs, and substantial capital investment (Das & Sharma, 2020; Zhou *et al*., 2010). Therefore, it is necessary to develop methods for treating saline surface water that are suitable for people in the Mekong Delta. Currently, studies on using adsorbents to treat water pollutants are of interest, and their application is quite simple, inexpensive, and does not require many pretreatment stages like other processes. Given the limitations of current technologies, research attention has increasingly shifted toward novel adsorbent materials, such as bismuth(III) oxide (Bi_2O_3), due to their unique properties and ease of application.

Bismuth(III) oxide (Bi_2O_3) was the most important compound in the industry for the bismuth specialty. This compound was the starting point for all bismuth compounds. In water treatment, Bi_2O_3 nanomaterials were also used to remove azo dyes and decompose Rhodamine B, Bi_2O_3, and to adsorb arsenic and bromide from water (Das & Sharma, 2020; Zhou *et al.,* 2010). Furthermore, studies on Bi_2O_3 as an adsorbent, such as its use for the removal of azo dyes in textile dyeing wastewater, indicate that Bi_2O_3, with its heterogeneous photocatalytic properties, is a potential solution for wastewater treatment (Christina, 2016). Furthermore, β- and α-Bi_2O_3 nanomaterials were synthesized by microwave-assisted synthesis for the photocatalytic removal of Rhodamine B (Huang *et al.,* 2011). Another study focused on bismuth nanoparticles for the treatment of heavy metals in wastewater.

In addition, while numerous studies have focused on developing materials for salinity removal, many existing processes for treating saline water are often criticized for being complicated, expensive, producing secondary pollutants, and using materials with limited durability. Furthermore, a gap remains in the literature regarding the application of Bi_2O_3 nanoparticles for the adsorption and removal of salinity from water environments. This lack of investigation suggests a promising new research direction and highlights the potential of Bi_2O_3 as a novel, cost-effective, and highly efficient adsorbent material for chloride and other pollutants. Therefore, the primary objective of

this study is to develop a practical and cost-effective adsorption method using synthesized Bi_2O_3 nanoparticles to reduce chloride concentrations in salt-affected surface water. This material-centric approach, focused on a sustainable water treatment solution, is expected to support the restoration of aquatic ecosystems and significantly improve water quality for surrounding communities affected by saltwater intrusion in regions such as Rach Gia City.

MATERIALS AND METHODS

Chemicals

Distilled deionized (DI) water was utilized for the synthesis of the Bi_2O_3 material, preparation of the aqueous NaCl stock solution, and all subsequent analytical procedures. The following pure chemicals were used as received: bismuth(III) nitrate pentahydrate ($Bi(NO_3)_3.5H_2O$, precursor); sorbitol ($C_6H_{14}O_6$, carrier/dispersion agent); sodium chloride (NaCl, adsorbate); sodium hydroxide (NaOH) and sulfuric acid (H_2SO_4), pH adjustment); silver nitrate ($AgNO_3$, titrant) and potassium chromate (K_2CrO_4, indicator for Mohr method); and potassium bromide (KBr, German source, used for FTIR analysis). All chemicals, except KBr, were sourced from China and distributed by Trung Son Technology Co., Ltd, Vietnam. Nitrogen gas (N_2) and liquid nitrogen (N_2 liquid) were sourced from Vietnam.

Material Preparation

Bi_2O_3 was fabricated using the solid dispersion evaporation technique (SDAT) with sorbitol as the carrier, as described by Shirkhanloo *et al.* (2017). Firstly, 5 g of bismuth nitrate ($Bi(NO_3)_3.5H_2O$) was mixed with a 70% sorbitol ($C_6H_{14}O_6$) solution, and 2 mL of DI water was added. The mixture was stirred for 20 min, then left in an ultrasonic tank for 20 min. Next, 10 mL of water was added, and the mixture was stirred at 110 °C and 100 rpm for 30 min. Meanwhile, the pH was adjusted to 7 without any precipitation. The mixture was then dried at 105 °C for 1 h and finally heated at 550 °C for 1 h to obtain a yellow nano-Bi_2O_3 product (as shown in Figure 1).

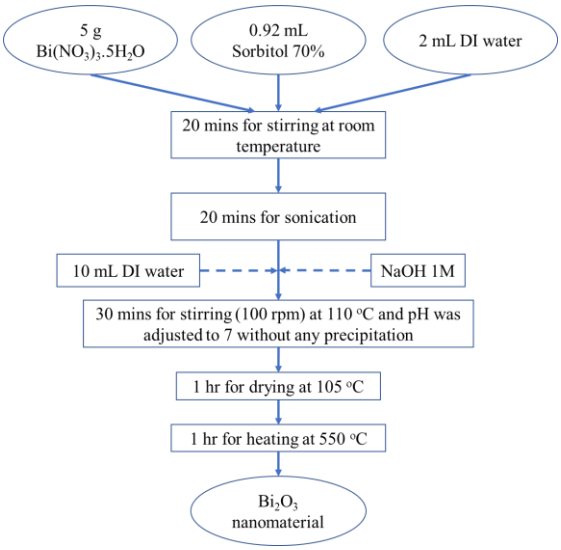


Fig. 1: Flowchart of the material synthesis research process

The saline water sample was collected near the Rach Gia sluice gate, Rach Gia city, Kien Giang province, Vietnam (currently Rach Gia ward, An Giang province, Vietnam). Figure 2 shows the location of the water sampling.

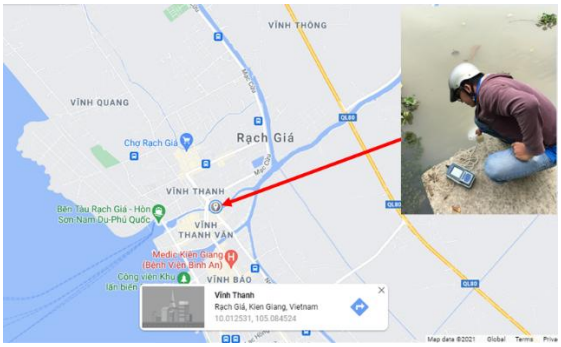


Fig. 2: Water sampling location

Characterization and Analysis

The characteristics of the material were determined for morphology and chemical composition by SEM-EDX (JCM 7000 Neo Scope, JOEL), functional groups by FTIR (Alpha, Bruker), surface area by BET (CBET 201A, PMI), and crystal phase by XRD (Aeris, Malvern Panalytical).

The surface water was collected in accordance with TCVN 6663-1:2011. Ion Cl^- was analyzed by the titration method of TCVN 6194-1996 using a UV-Vis spectrophotometer (Specord 2010, Analytik Jena), and the pH of the solution was determined by a pH meter (sensION+ PH3, Hach).

Chloride Adsorption Experiment

This section details the systematic investigation of independent variables affecting chloride adsorption in synthetic saline water samples, followed by the determination of appropriate adsorption conditions for the material, and then testing on actual saline water samples.

The compositions of the saline waters were referenced in Table 1. The experiments were conducted by adding 50 mg of Bi_2O_3 material into 50 mL of 70 mg/L NaCl solution, which was then shaken at 120 rpm for a range of time (5 min, 10, 15, 30, 45, 60, 90, and 120 min). After that, the solution was filtered through a Newstar filter paper (Φ11 µm), and the chloride concentration was analyzed. Various conditions of pH conditions (pH 2 - 9, ± 1), material dosages (50 - 120 mg/50 mL, ± 10 mg), and initial chloride concentrations (10, 50, 70, and 100 mg/L), and temperatures (20, 30, and 40 °C) were investigated. The point of zero charge of the material was measured by titration, with an initial pH range of 2-9 (Nguyen *et al.,* 2022). Finally, the optimal value of pH, time, and temperature would be applied to real saline surface water collected from Rach Gia city for a practical application test. After adsorption, the material was mixed with 1 M NaOH solution in the ratio 1:1 (g of material/L of solution) and stirred well for 60 min before being rinsed with deionized water to pH ~ 7. The experiment was replicated 10 times to ensure consistent results. The chloride in the solution was determined before and after adsorption to evaluate the adsorption capacity after each regeneration.

The following equation calculates the chloride adsorption capacity (q, mg/g):

$$q = \frac{C_0 - C_t}{m} \times V \quad (1)$$

Table 1. Chemical compositions of surface water in Rach Gia city

Collected area	Water quality parameters							
	pH	**TSS** ***(mg/L)***	**Salinity** ***(‰)***	**Total Fe** ***(mg/L)***	**COD** ***(mg/L)***	**NO_3-N** ***(mg/L)***	**NO_2-N** ***(mg/L)***	**Chloride** ***(mg/L)***
Cai San Canal – Rach Soi market	6.28	34.00	0.20	0.43	33.00	0.6	0.48	112.00
Dau Voi – Rach Gia canal to Long Xuyen, Vinh Thong ward	6.91	48.00	0.20	1.33	24.50	0.3	0.17	131.00
Rach Gia canal to Long Xuyen, Phi Thong commune	6.95	31.00	0.20	1.17	24.50	0.34	0.17	101.00
1st bridge	6.98	40.00	0.20	0.35	21.00	0.24	0.16	112.00

where C_0 and C_t are chloride concentrations in the solution at the beginning and at time t ($mgCl^-/L$). m is the mass of Bi_2O_3 adsorbent (g), and V is the volume of the solution (L).

Kinetic models are used to study the kinetics of metal ion adsorption onto solid materials in aqueous media, including pseudo-first-order, pseudo-second-order, and intraparticle diffusion. For the adsorption of molecules or ions in a liquid solution by a solid material, adsorption was usually described by the Langmuir and the Freundlich isotherm equations. The objective of these models was to determine the adsorption capacity, the mechanism of chloride ion adsorption onto the adsorbent, and the adsorbent-chloride ion affinity. The Langmuir equation is described in Eq. (2), while the Freundlich isotherm equation is described in Eq. (3)

$$q_e = q_m \times \frac{K_L \times C_e}{1 + K_L \times C_e} \quad (2)$$

$$\ln q_e = \ln K_F + \frac{1}{n} \times \ln C_e \quad (3)$$

where q_m is the maximum adsorption capacity (mg/g), and q_e is the adsorption capacity at equilibrium (mg/g). C_e is the effluent concentration at equilibrium (mg/L), and K_L is the Langmuir adsorption constant (L/mg). K_F (L/g) and 1/n are Freundlich constants.

RESULT AND DISCUSSION

Characterization of Bismuth (III) Oxide

The morphology of bismuth (III) oxide captured by SEM is exhibited in Figure 3(a). In general, the nanoparticle bismuth oxide has a spherical or circular shape. BET calculated the surface area to be about 14.34 m^2/g, which was consistent with previous reports for Bi_2O_3 nanoparticles of 7-29 m^2/g (Schlesinger, Schulze, *et al.,* 2013; Schlesinger, Weber, *et al.,* 2013). As shown in Figure 3(b-c), EDX analysis determined the elemental composition of the Bi_2O_3 material before and after chloride adsorption. The common elements of Bi_2O_3 are C (44.24%), O (26.90%), and Bi (28.86%). After chloride adsorption, the Bi content decreased to 14.33%, while Cl was detected at 1.86%, confirming the successful adsorption of Cl on the Bi_2O_3 surface.

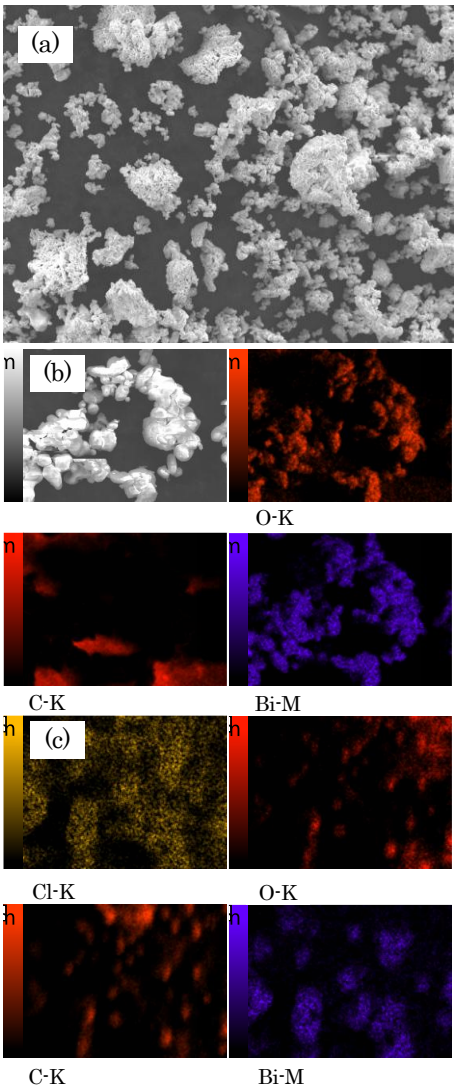


Fig. 3: SEM images of Bi_2O_3 (a) and EDX-mapping results of Bi_2O_3 (b) before and (c) after chloride adsorption

The XRD pattern of the Bi_2O_3 material is plotted in Figure 4(a), showing the existence of peaks at 2θ of 25.6°, 27.5°, 33°, 46.4°, and 52° of the (002), (121), (202), (221), and (321)

planes, respectively, of Bi_2O_3 crystals. The average crystal size of Bi_2O_3 in this study was 12 nm, which is smaller than the 40 nm reported for Bi_2O_3 nanoparticles in previous studies (Shirkhanloo *et al.,* 2017) or the > 100 nm reported for Bi2O3 nanoparticles in another study (Mallahi & Vaezi). The FTIR spectra of Bi_2O_3 materials before and after chloride adsorption are presented in Figure 4(b). The peak at a wavenumber of about 3500 cm^{-1} is typical of the O-H bond of adsorbed water on the material (Oudghiri-Hassani *et al.,* 2015). The NO_3 group is identified at 1370 and 840 cm^{-1} (Trivedi *et al.,* 2015). Moreover, the peaks around 700 to 400 cm^{-1} are the Bi-O binding. In particular, the peak at 1400 cm^{-1} in the FTIR spectrum of the material after chloride adsorption is typical of the Bi-Cl bond (Trivedi *et al.,* 2015), indicating that the chloride ion was successfully adsorbed on the surface of the Bi_2O_3 material.

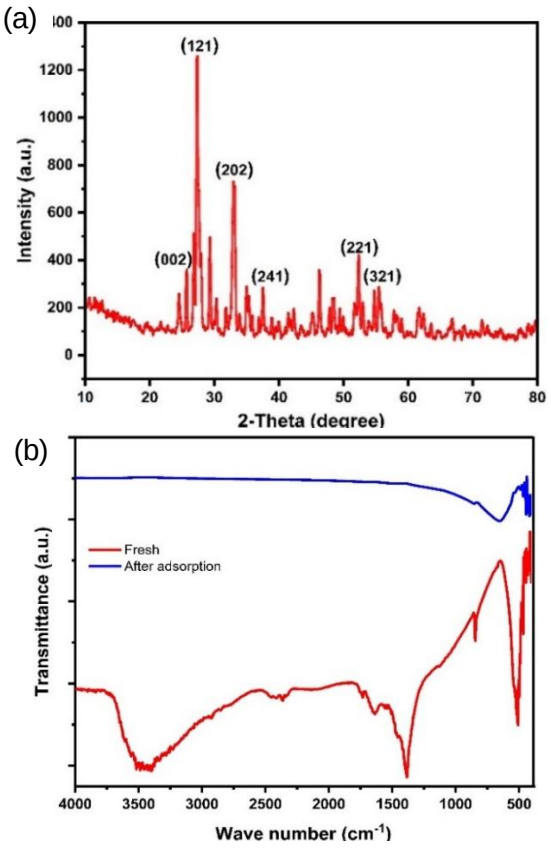


Fig. 4: (a) XRD pattern and (b) FTIR spectrum of Bi_2O_3

Adsorption of Chloride

The results of the pseudo-first-order, pseudo-second-order, and intraparticle diffusion models are illustrated in Table 2. Among these kinetic models, the chloride adsorption capacity was best described by the pseudo-second-order model, with the highest correlation coefficient (R^2) of 0.9898. The theoretical chloride adsorption capacity calculated by this model equation was determined to be q_{eT} = 34.48 mg/g, which is close to the experimental chloride adsorption capacity (q_{eE} = 30.73 mg/g).

The Langmuir and the Freundlich isotherm models were used to evaluate and describe the adsorption process, as described in Table 3. The results of both models were suitable for the chloride adsorption process of Bi_2O_3 materials. However, the Freundlich model was more acceptable due to its higher R^2 value, indicating that the material surface is homogeneous and has the same affinity for chloride ions at all points, with only individual ion interaction. Furthermore, it forms a monolayer on the material surface, mainly via physical adsorption. Therefore, the dosage of materials should be increased to enhance their adsorption capacity. The Freundlich parameter n in the isotherm equation is in the range 1-10, indicating that the research material was suitable for the adsorption process.

Table 2. Kinetic equations of chloride adsorption by Bi_2O_3 material

Model	Linear form of equation	R^2	Theoretical q_{eT} ($mgCl^-/g$)
Pseudo-first-order	y = -0.0204x + 2.8301	0.82	49.02
Pseudo-second-order	y = 0.029x + 0.4207	0.99	34.48
Intraparticle diffusion	y = 0.6369x + 0.5545	0.91	-

Table 3. The parameter of the adsorption isotherm model

Isotherm	Parameter	Temperature		
		20°C	30°C	40°C
Langmuir	Q_{max} (mg/g)	38.46	46.10	49.26
	K_L (L/mg)	0.09	0.09	0.17
	R^2	0.95	0.97	0.99
Freundlich	K_f (mg/g)(L/mg)^n	0.24	0.20	0.14
	N	1.74	2.52	1.68
	R^2	0.99	0.99	0.97

As shown in Figure 5(a), the chloride adsorption capacity increased rapidly over the first 60 min and reached equilibrium after 90 min. This can be explained as follows: in the first 60 min, the number of chloride ions bound to the material remains low. Hence, the affinity between the adsorption centers and the surrounding chloride ions remains strong. This situation led to rapid adsorption. After that, the number of chloride ions on the material surface became denser and slowly reached saturation after 90 min, after which the adsorption capacity remained constant. This is similar to the results reported in the literature when using Bi_2O_3 for RhB (110 min, (Schlesinger, Weber, *et al.*, 2013)) or As(III) adsorption (120 min, (Balint *et al.*, 2021)).

Regarding the effect of solution pH, the results in Figure 5(b) demonstrate that Bi_2O_3 materials exhibit high adsorption capacity at pH 3-5, with a maximum of 40.89 mg/g at pH 4. At pH > 4, the concentration of anion OH^- gradually increased, thus leading to competition between anion Cl^- and OH^- for the adsorption site. At pH < 4, the nanoparticles tend to be dissolved, thereby reducing their adsorption capacity (Shi *et al.*, 2017). The surface charge of Bi_2O_3 materials was greatly affected by the pH of the chloride solution. The pH_{zpc} value of the material was determined at ~ 8.2 (inset of Figure 5(b)). At pH < pH_{zpc}, the material surface was positively charged, and chloride adsorption occurred via an electronic interaction mechanism. However, at pH > pH_{zpc}, the adsorption capacity decreased due to the material's negatively charged surface and the competitive adsorption of OH^- ions. These results are consistent with those of Shi *et al.* (2017), who used a Bi_2O_3 nanomaterial with a pH_{zpc} of 8.38 for bromide adsorption.

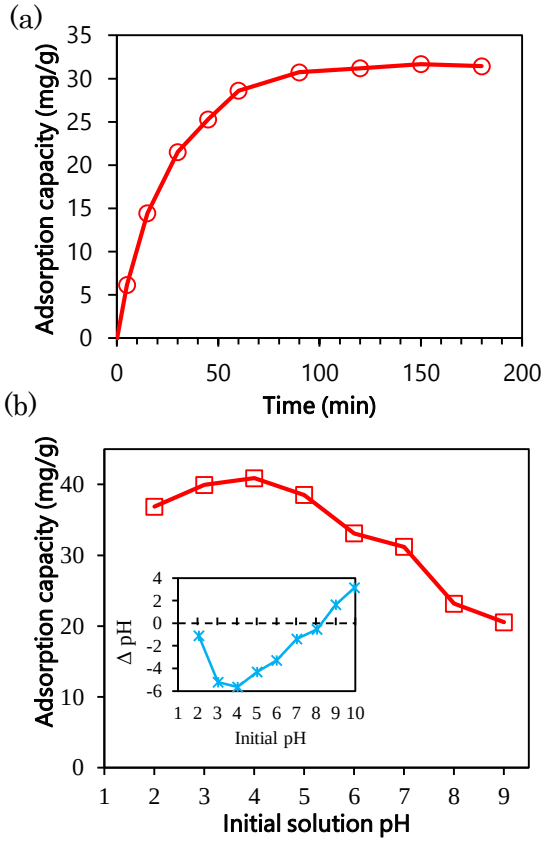


Fig. 5: Effect of (a) contacting time and (b) initial solution pH on chloride adsorption capacity

In addition to adsorption time and pH, the material dosage also affected the chloride adsorption capacity. The results in Figure 6(a, b) illustrate that the amount of material dosage strongly influenced the chloride adsorption capacity, and it was inversely proportional to the material dosage. Preliminary results indicate that at 50 mg of adsorbent, the highest adsorbed chloride content is 30.02 mg/g.

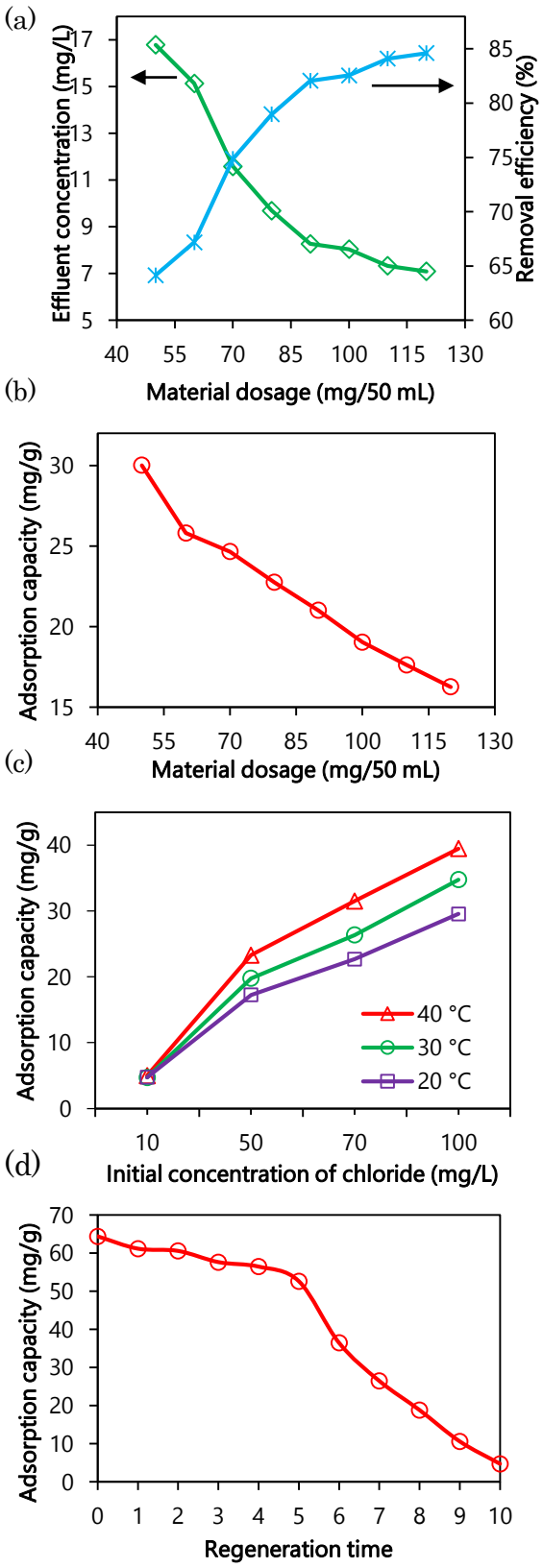


Fig. 6: Effect of (a, b) Bi_2O_3 dosage and (c) initial concentration and temperature on chloride adsorption; and (d) the chloride adsorption capacity after 10 cycles

Both initial concentration and temperature affect the adsorption capacity of chloride (Figure 6(c)). There is a tendency for adsorption capacity to increase with higher initial chloride concentration and higher ambient temperature. The higher the initial chloride concentration, the more interaction between the chloride ions and the adsorption centers on the surface of the material. Also, as the temperature increased, the chloride ions in the solution became more active. This led to collisions between the material surface and ions, similar to other works in the literature (Balint *et al.*, 2021; Shi *et al.*, 2017).

The durability and stability of the material were also tested for 10 cycles of adsorption-regeneration (Figure 6(d)). The results show that the chloride adsorption gradually decreased after 10 regeneration cycles, from 64 $mgCl^-/g$ to 5 $mgCl^-/g$. This trend could be explained by the incomplete desorption of chloride adsorbed on the material surface. Balint *et al.* (2021) concluded that Bi_2O_3 nanomaterials could be regenerated and reused to remove As from the solution after 4 regeneration cycles.

Table 4. Chloride removal efficiency of the material after regeneration

Number of cycles	Before chloride concentration (mg/L)	After chloride concentration (mg/L)	The percent of removal (%)
0	541.48	412.73	23.78
1	564.41	442.12	21.67
2	560.88	439.77	21.59
3	560.88	445.65	20.55
4	560.88	448.00	20.13
5	559.12	453.88	18.82
6	539.72	466.82	13.51
7	539.72	486.81	9.80
8	539.72	502.09	6.97
9	539.72	518.55	3.92
10	539.72	530.31	1.74

CONCLUSIONS

Bi_2O_3 nanomaterials were successfully synthesized and applied with excellent efficiency in chloride adsorption. The optimum conditions for adsorption were determined to be a contacting time of 90 min and a solution pH of 4, yielding a maximum adsorption capacity of 40.89 mgCl^-/g in the synthetic saline solution. Mechanistic studies indicated that chloride adsorption on the surface of the bismuth oxide material was predominantly physical adsorption, with the kinetic process being rapid and well described by the pseudo-second-order model. The practical application test showed that the Bi_2O_3 material achieved chloride removal efficiency of 22.76% when applied to the original saline surface water sample collected from Rach Gia city. This represents a promising initial result and demonstrates material activity in a complex, real-world matrix. Future research should focus on the in-depth effects of coexisting ions and on long-term reusability under continuous-flow conditions to further validate the practical applications of the Bi_2O_3 material.

ACKNOWLEDGEMENT

Vietnam National University – Ho Chi Minh City funds this research under grant number DS2025-16-01. We acknowledge Ho Chi Minh City University of Technology (HCMUT) and An Giang University (AGU), VNU-HCM, for their contributions to the study.

REFERENCES

Balint, R., Bartoli, M., Jagdale, P., Tagliaferro, A., Memon, A. S., Rovere, M., and Martin, M., 2021. "Defective bismuth oxide as effective adsorbent for arsenic removal from water and wastewater." *Toxics, 9(7)*, 158. https://doi.org/10.3390/toxics9070158

Be, N. V., Trien, T. V., Tri, V. P. D., and Hang, T. T. L., 2017. "Impacts of saline intrusion on agriculture and aquaculture in the Tran De district, Soc Trang province." *CTU J. Sci., 50*, 94-100. https://doi.org/10.22144/ctu.jvn.2017.071

Be, T. T., Sinh, B. T., and Miller, F., 2007. Challenges to sustainable development in the Mekong Delta: Regional and national policy issues and research needs: Literature analysis, Sustainable Mekong Research Network (Sumernet)., Vietnam

Binh, N. T., Phanh, T. S., and Huan, L., 2012. "Participatory vulnerability analysis: A case study from saline intrusion in the Mekong Delta." *CTUJ. Sci., 24(b)*, 229-239.

Christina, P. J. D., 2016. Preparation of Bi_2O_3 nanostructures and their light driven catalytic activity towards the erasure of textile dyes. Final Year Project, Universiti Tunku Abdul Rahmam, Malaysia.

Dao, N. V., and Binh, P. T. T., 2019. "Evaluation of the situation and impact of climate change on the salinity intrusion at Ben Tre province." *J. Hydrometeorol., 700*, 12-22.

Das, T. R., and Sharma, P. K., 2020. "Bimetal oxide decorated graphene oxide (Gd_2O_3/Bi_2O_3@GO) nanocomposite as an excellent adsorbent in the removal of methyl orange dye." *Mater. Sci. Semicond. Process, 105*, 104721. https://doi.org/10.1016/j.mssp.2019.104721

Hoa, N. M., Giang, N. H., Tung, T. S., and Guong, V. T., 2016. "Salinisation of soil

and water on agricultural and aquacultural systems in Binh Dai district, Ben Tre province," *CTU J. Sci., 42*, 40-49.

Huang, Q., Zhang, S., Cai, C., and Zhou, B., 2011. "β- and α-Bi_2O_3 nanoparticles synthesized via microwave-assisted method and their photocatalytic activity towards the degradation of rhodamine B." *Mater Lett., 65(6)*, 988-990. https://doi.org/10.1016/j.matlet.2010.12.055

Mallahi, M., and Vaezi, M. "Synthesis and characterization of bismuth oxide nanoparticles via sol-gel method." *Am. J. Eng. Res., 3(4),* 162-165.

Nguyen, T. T., Le, T. T., Nguyen, T. B. T., Thi, T. N., Tran, L. B., Nguyen, T. Q. A., and Nguyen, N. H. 2022. "Effect of pH on the performance of $Bi_2O_2CO_3$ nanoplates for methylene blue removal in water by adsorption and photocatalysis." *Bull. Chem. React. Eng. Catal., 17(2)*, 331-339. https://doi.org/10.9767/bcrec.17.2.13370.331-339

Oudghiri-Hassani, H., Rakass, S., Al Wadaani, F. T., Al-ghamdi, K. J., Omer, A., Messali, M., and Abboudi, M. 2015. "Synthesis, characterization and photocatalytic activity of α-Bi_2O_3 nanoparticles." *J. Taibah Univ. Sci., 9(4)*, 508-512. https://doi.org/10.1016/j.jtusci.2015.01.009

Phuong, N. M., Verplancke, H., Khoa, L. V., and Guong, V. T. 2009. "Physical soil degradation on intensive rice cultivation areas in the Mekong Delta and the effects of crop rotation on aggregate stability of paddy soil." *CTU J. Sci., 11(a)*, 194-199.

Queensland Government, 2013. Impacts of salinity. https://www.qld.gov.au/environment/land/management/soil/degradation/salinity/impacts

Rahaman, M. A., Rahman, M. M., and Nazimuzzaman, M. 2020. Impact of salinity on infectious disease outbreaks: experiences from the global coastal region. In W. Leal Filho, T. Wall, A. M. Azul, L. Brandli, & P. G. Özuyar (Eds.), *Good Health and Well-Being*, Springer International Publishing, Cham. pp. 415-424).

Schlesinger, M., Schulze, S., Hietschold, M., and Mehring, M. 2013. "Metastable β-Bi_2O_3 nanoparticles with high photocatalytic activity from polynuclear bismuth oxido clusters." *Dalton Trans., 42(4)*, 1047-1056. https://doi.org/10.1039/C2DT32119J

Schlesinger, M., Weber, M., Schulze, S., Hietschold, M., and Mehring, M. 2013. "Metastable β-Bi_2O_3 nanoparticles with potential for photocatalytic water purification using visible light irradiation." *ChemistryOpen, 2(4)*, 146-155. https://doi.org/10.1002/open.201300013

Shi, M., Guo, C., Li, J., Li, J., Zhang, L., Wang, X., Ju, Y., Zheng, J., and Li, X. 2017. "Removal of bromide from water by adsorption on nanostructured δ-Bi_2O_3." *J. Nanosci. Nanotechnol., 17(9)*, 6951-6956. https://doi.org/10.1166/jnn.2017.14473

Shirkhanloo, H., Safari, M., Amini, S. M., and Rashidi, M. 2017. "Novel semisolid design based on bismuth oxide (Bi_2O_3) nanoparticles for radiation protection." *Nanomed. Res. J., 2(4)*, 230-238. https://doi.org/10.22034/nmrj.2017.04.004

Trivedi, M. K., Branton, A., Trivedi, D., Nayak, G., Bairwa, K., and Jana, S. 2015. "Spectroscopic characterization of disodium hydrogen orthophosphate and

sodium nitrate after biofield reatment." *J. Chromatogr, Sep. Tech., 6(5)*, 1000282. http://dx.doi.org/10.4172/2157-7064.1000282

Vengosh, A. 2014. 11.9 - Salinization and saline environments. In H. D. Holland & K. K. Turekian (Eds.), *Treatise on Geochemistry 2nd Eds.*, Elsevier, Oxford, pp. 325-378.

Vo, T. A. N., and Son, T. Q. T. 2022. "Impacts of saltwater intrusion on crop yield in the Mekong River Delta." *J. Vietnam Agric. Sci. Technol., 03(136)*, 24-33.

Zhou, L., Gao, C., and Xu, W. 2010. "Magnetic dendritic materials for highly efficient adsorption of dyes and drugs," *ACS Appl. Mater. Interfaces, 2(5)*, 1483-1491. https://doi.org/10.1021/am100114f